Surface-Directed Spinodal Decomposition in Binary Fluid Mixtures

Sorin Bastea[1,†], Sanjay Puri[2] and Joel L. Lebowitz[1]

[1] *Department of Mathematics and Physics, Rutgers University, New Brunswick, NJ 08903, USA*

[2] *School of Physical Sciences, Jawaharlal Nehru University, New Delhi 110067, INDIA*

Abstract

We consider the phase separation of binary fluids in contact with a surface which is preferentially wetted by one of the components of the mixture. We review the results available for this problem and present new numerical results obtained using a mesoscopic-level simulation technique for the 3-dimensional problem.

PACS numbers: 64.75.+g, 61.30.Hn, 68.08.Bc, 47.70.Nd

I. INTRODUCTION

There has been much interest in the phase-separation dynamics of homogeneous binary mixtures, which have been rendered thermodynamically unstable by a rapid quench below the coexistence curve. The time evolution of pure bulk mixtures in which the evolving system coarsens into domains rich in either of the components is now reasonably well-understood. These domains are characterized for late times by a single length scale $L(t) \sim t^{\phi}$, where t is the time and the growth exponent ϕ depends upon the system considered, e.g., whether or not the order parameter is conserved, the relevance of hydrodynamic effects, etc. [1].

An experimentally important variation of this problem considers the role of surfaces with a preferential attraction for one of the components of the mixture. The first experimental study of this problem is due to Jones *et al.* [2], who considered unstable polymer mixtures of polyethylene-propylene (PEP) and perdeuterated PEP (d-PEP) in a thin-film geometry. The surface energy of d-PEP is somewhat less than that of PEP leading, in addition to bulk phase separation (spinodal decomposition), to a preferential deposition of d-PEP at any free surface. Jones *et al.* studied laterally-averaged composition profiles as a function of distance from the surface. The bulk is characterized by randomly-oriented phase-separation profiles and the lateral averaging procedure does not yield a systematic behavior. However, the surface exhibits an enrichment layer in the preferred component, which is followed by a depletion layer. This oscillatory profile is time-dependent and decays with a characteristic length to the bulk composition.

This experiment motivated many further investigations of this problem. The experimental techniques and results have been reviewed by Krausch [3], and the theoretical and numerical developments by Puri and Frisch [4] and Binder [4]. To date, most numerical studies of this problem have focused on the case of binary mixtures without hydrodynamic effects, i.e., the growth of surface wetting layers and bulk domains is governed by diffusive processes. However, many important experiments in this area involve binary fluids in contact with a surface. It is well-known that macroscopic matter and energy flows, i.e., hydrody-

namic effects, drastically alter the nature of domain growth in the bulk phase-separation problem. Therefore, it is reasonable to expect important physical effects to result from hydrodynamic flows in the case of surface-directed phase-separation also. To understand some of the issues involved, we have undertaken a detailed numerical simulation of this problem. In particular we adapted mesoscopic models formulated to study bulk spinodal decomposition in binary fluids to surface-directed spinodal decomposition.

This paper is organized as follows. Section 2 reviews available experimental, analytical and numerical results for this problem. In Section 3, we describe our model and the numerical methods used. These involve an "integration" of the Vlasov-Boltzmann equations for the binary mixture in contact with a surface. In Section 4, we present results obtained from our simulations. Finally, Section 5 is devoted to a summary and discussion of the results.

II. SUMMARY OF AVAILABLE RESULTS

A. Experimental Studies

One of the earliest experiments on phase-separating binary fluids near a surface is due to Guenoun *et al.* [6], which considered unstable mixtures of cyclohexane (C) and methanol (M) in contact with a surface which preferred M. The surface rapidly developed a M-rich layer, followed by a bicontinuous domain structure. Guenoun *et al.* found that domain growth was characterized by a number of different length scales. Thus, the wetting layer grew as $R_1(t) \sim t^a$ with $a \simeq 0.56$. The domains adjacent to the wetting layer were anisotropic and were characterized by perpendicular ($L_\perp(t) \sim t^b$ with $b \simeq 0.64$) and parallel ($L_\parallel(t) \sim t^c$ with $c \simeq 1$) scales.

Wiltzius *et al.* [7] considered critical fluid mixtures of polyisoprene (PI) and PEP sealed between two quartz plates. They found that the structure factor exhibited two peaks - one corresponding to the usual bulk domain length scale $L_b(t) \sim t$ and the other corresponding to a fast length scale $L_s(t) \sim t^{3/2}$. Furthermore, they found that the dimensionality of

domain growth associated with the fast length scale was $d = 2$, suggesting that it resulted from a rapid coarsening in the surface layer. The rapid surface growth was interpreted as a prelude to the formation of a complete wetting layer on the surface. In that case, there is no inconsistency between their results and the earlier results of Guenoun *et al.* [6], which correspond to later times when a complete wetting layer was already formed. Similar experiments were also performed by Shi and collaborators [8] on mixtures of guaiacol and glycerol-water confined in a thin-film geometry.

Detailed studies of the morphologies which arise for phase-separating mixtures confined to 1- and 2-dimensional capillaries were performed by Tanaka and co-workers [9] on critical and off-critical mixtures of polyvinyl-methyl-ether (PVME) and water, and ϵ-caprolactone oligomer (OCL) and styrene oligomer (OS). In particular, they clarified conditions under which the equilibrium state is completely wet (i.e., only the preferred phase is in contact with the surface) or partially wet (i.e., both phases are in contact with the surface). Tanaka's group did not observe the fast growth reported by Wiltzius and co-workers [7,8], possibly because the quench depth in their experiments was too large. Once the wetting layer is formed, they found that its thickness grows linearly in time, i.e., $R_1(t) \sim t$, in disagreement with the experiments of Guenoun *et al.* [6]. In most of their experiments, the wetting layer is finally destabilized by a Rayleigh instability and the system crosses over to a partially wet morphology.

B. Analytical Arguments

The equilibrium behavior of immiscible binary fluids in contact with a substrate was examined long ago by Young [10]. Let γ_A and γ_B be the surface energies per unit area for the fluids A and B in contact with the substrate (say, $\gamma_B > \gamma_A$); and let σ be the surface tension between fluids A and B. Then, the contact angle θ between A and the surface is given by $\sigma \cos\theta = \gamma_B - \gamma_A$. This equation has no solution when $(\gamma_B - \gamma_A)/\sigma > 1$, which corresponds to a situation where the preferred fluid (A) completely wets the substrate. The

effects of geometry and composition can also be included [9,11,12].

The nonequilibrium problem we consider is a homogeneous critical binary mixture (at high temperature) in contact with a surface which has a preference for one of the components of the mixture. At time $t = 0$ the system is quenched below its critical temperature and becomes unstable to phase separation. We are interested in the dynamics of approach to the equilibrium morphology, which will consist of either partially wet (PW) or completely wet (CW) configurations. Typically, the surface is initially coated by the preferred component, which is then followed by the growth of the wetting layer [9]. We focus here on the wetting layer growth.

As remarked by Siggia [5] the bicontinous morphology of critical or near critical phase separating binary fluids consists essentially of interpenetrating "tubes". When a tube of the preferred phase establishes contact with the surface layer the curvature induced pressure gradient σ/L^2 leads to a flow of material from the tube to the surface. The material flux per tube can be estimated for example from Poiseuille law to be $(\sigma/\eta)L^2$ [5]. Then $S(dR_1/dt) \sim (\sigma/\eta)L(t)^2 \times (S/L(t)^2)$, where S is the surface area and $S/L(t)^2$ is the number of tubes. Thus, $R_1(t) \sim (\sigma/\eta)t$ for the hydrodynamic problem, a result which has been confirmed experimentally [9]. We believe that the discrepancy between this result and the earlier experimental work of Guenoun *et al.* [6] is due to the long-lived transient growth laws dependent upon the form of the surface potential [13]. For the diffusive case the chemical potential gradient between the bulk tube, $\mu \sim (\sigma/L)$ [1], and the flat tube portion at the surface, $\mu \sim 0$, induces a current $j \sim (\sigma/L^2)$ and therefore a flux per tube $\sim \sigma$. The corresponding growth law is then $R_1(t) \sim \sigma^{1/3}t^{1/3}$.

The wetting layer grows until it reaches the equilibrium length (dictated by the composition for a CW morphology), or is destabilized by surface fluctuations and goes over to the appropriate equilibrium PW morphology. There is also a dynamical coupling of phase separation and the growth of the wetting layer, which leads to the domains adjacent to the wetting layer being anisotropic with $L_\perp(t) < L_\parallel(t)$ [6,4].

C. Numerical Results

One of the earliest numerical studies of the hydrodynamic problem is due to Keblinski *et al.* [15], who performed molecular dynamics (MD) simulations of binary fluids (AB) confined in a 2-dimensional capillary (or a planar thin film). One of the cases that they study is when the wall preferentially attracts A, which is analogous to the experiments we have discussed earlier. In this case they observe a "fast mode" in the surface layer but with an exponential growth rather than the power law growth.

Chen and Chakrabarti [16] have studied phase separation in 2-dimensional binary fluids near a surface through numerical solutions of the coarse-grained model H equations [1] in a semi-infinite geometry. The model H equations consist of coupled dynamical equations for the order parameter and the fluid velocity field. Chen and Chakrabarti consider a surface with a long-range attraction for one of the components of the mixture and impose "no-slip" conditions on the velocity field at the surface. They find that the wetting-layer growth crosses over from $R_1(t) \sim t^{1/3}$ (characteristic of bulk diffusive growth in any dimension) to $R_1(t) \sim t^{2/3}$ (characteristic of bulk hydrodynamic growth in $d = 2$). This crossover is associated with domains of the preferred component establishing contact with the surface layer and their subsequent rapid draining into the surface layer.

Another study of model H in a semi-infinite geometry is due to Tanaka and Araki [17]. These authors solved the model H equations numerically in $d = 3$. They find that the wetting-layer thickness grows initially as $R_1(t) \sim t^{1/3}$ (characteristic of diffusive growth) and then crosses over to the hydrodynamic regime with $R(t) \sim t$. They also study characteristic length scales in the layer parallel to the surface. Far from the surface, they find the expected bulk growth law $L_\parallel(t) \sim t$, while in the vicinity of the surface they find a faster growth. However, it seems difficult to unambiguously assign an exponent to this faster growth. Furthermore, the time-regime of the "fast mode" is considerably later than the time-scale of formation of the complete wetting layer. This suggests to us that the "fast growth" observed by Tanaka and Araki should be identified with the anisotropic growth (with $L_\perp < L_\parallel$) of

domains in the vicinity of the wetting layer due to orientational effects of the wetting layer, rather than the "fast mode" of Wiltzius and others [7,8]. As we have discussed earlier, this fast mode is associated with the coating dynamics which results in a complete wetting layer.

Finally, we mention a MD study by Toxvaerd [18] who investigated critical mixtures (AB) of particles interacting through Lennard-Jones potentials. He focused on the morphologies which arise for different wall-types, e.g., one wall attracts A whereas the other wall attracts B versus the case where both walls attract A and B equally, etc. Using MD simulation he finds that the system evolves into a layered morphology, with the layer being parallel to the surface walls. We believe that these are metastable configurations which evolve exceedingly slowly due to the low effective dimensionality ($d = 1$) of the system.

The paucity of detailed numerical results for binary fluids undergoing phase separation in contact with a wetting surface motivated us to undertake a mesoscopic-level simulation of this problem, through a direct "solution" of the relevant Vlasov-Boltzmann equations.

III. DESCRIPTION OF MODEL

The subtle interplay between diffusion and convection which occurs in phase-separating fluids makes the modeling of these systems more complicated than that of solids. The local conservation of linear momentum and energy, which is characteristic of fluids, and the associated transport of matter and energy on macroscopic scales, plays a crucial role during phase segregation. Typically, the phase separation of binary fluids has been modeled either (a) at the microscopic level, e.g., via MD simulations, or (b) at the macroscopic level via coarse-grained hydrodynamic equations. An alternative to these approaches was introduced in Ref. [19]. The system studied was a binary mixture consisting of A and B particles with short range repulsive interactions, modeled by hard spheres with equal mass m and diameter d, and a long-range Gaussian repulsion between the two components, A and B. The dynamics was described by coupled Vlasov-Boltzmann kinetic equations:

$$\frac{\partial f_i}{\partial t} + \mathbf{v} \cdot \frac{\partial f_i}{\partial \mathbf{r}} + \frac{\mathbf{F}_i}{m} \cdot \frac{\partial f_i}{\partial \mathbf{v}} = J[f_i, f_1 + f_2] \qquad i = 1, 2 \tag{1}$$

where $f_i(\mathbf{r},\mathbf{v},t)$ are the one-particle distribution functions, $\mathbf{F}_i(\mathbf{r},t) = -\nabla V_i(\mathbf{r})$, $V_i(\mathbf{r}) = \int V(|\mathbf{r}-\mathbf{r\prime}|)n_j(\mathbf{r\prime})d\mathbf{r\prime}$ (Vlasov potential), $n_j(\mathbf{r\prime}) = \int f_j(\mathbf{r\prime},\mathbf{v},t)d\mathbf{v}$, with $i \neq j$, and $J[f,g]$ is the Boltzmann collision operator for hard core interactions [20]. The Boltzmann equation properly describes the dynamics of dilute gases, where the free flow of the particles is interrupted by localized binary collisions between particles that are uncorrelated. The Vlasov term takes into account the long-range interaction in the spirit of the mean-field approximation: each particle now moves between collisions in the background potential generated by all the other particles it is interacting with through the long-range potential $V(r)$.

The above mesoscopic representation in terms of one-particle distribution functions has the advantage that the relevant conservation laws are automatically satisfied, and it also provides a rigorous route to a macroscopic description [21]. Computationally, the method introduced in Ref. [19,22] to simulate the Vlasov-Boltzmann kinetics at the particle level, i.e., coupling of the direct simulation Monte Carlo (DSMC) algorithm [23] for close-range collisions and the grid-weighting method for the long-range repulsions [24], contains the essential physical ingredients of the Vlasov-Boltzmann equations, and it permits the study of much bigger systems than those used in MD calculations.

In the present work, we modify the model of Ref. [19] to include the presence of a preferred surface. One of the components of the binary mixture (say, A) interacts with the surface located at $z = 0$ through an attractive potential $W(z)$, which decays as z^{-3} at large distances, i.e., $W(z) = -W_0$ if $z \leq r_0$ and $-W_0(r_0/z)^3$ otherwise, where $W_0 > 0$. This interaction potential corresponds to the case of non-retarded van der Waals interactions in $d = 3$ [25]. The wall is diffusive [26], i.e., particles "hitting" the wall are absorbed and re-emitted isotropically with a velocity drawn from a Maxwellian distribution with the temperature of the wall, T_W. The other wall along the z direction is purely reflective (no preferred attraction), which allows us to run the simulations for longer times than if the set-up was symmetric. We performed simulations with equal fractions of the components at fixed temperature, $T/T_c = 0.6$, $T_W = T$, where T_c is the bulk mean-field critical temperature of the system, using the velocity-rescaling technique introduced by Berendsen *et al.* [27]. Below

T_c the bulk fluid segregates into an A rich and a B rich components, denoted by 1 and 2 respectively. The parameter varied was the strength of the wall-particle interaction W_0.

As discussed in subsection 2.2, the wall-wetting morphology, i.e., completely wet (CW) versus partially wet (PW), is determined by the ratio $\sigma/(\gamma_2 - \gamma_1)$, where σ is the surface tension between the two fluid phases 1 and 2; and γ_1, γ_2 are the corresponding wall-fluid surface tensions. Taking into account that A and B are partially miscible the surface tension parameters can be estimated as follows. Consider the A-rich phase (1) with average total particle density n_0 and average individual densities n_{1A}^0 and n_{1B}^0, $n_0 = n_{1A}^0 + n_{1B}^0$. The wall-fluid surface energy is then

$$\gamma_1 = \int_0^\infty dz n_{1A}(z) W(z) \tag{2}$$

If we neglect the inter-particle spatial correlations, which is appropriate in our model if the long-range repulsion between the two components is sufficiently weak, we can write $n_{1A}(z) = n_{1A}^0 \exp[-\beta W(z)]$. With this assumption and using the fact that the phases are symmetric, we obtain the expression

$$\gamma_2 - \gamma_1 = k_B T n_0 \phi_0 r_0 H(\beta W_0), \tag{3}$$

where $\pm\phi_0$ is the average order parameter in the two phases, $\phi_0 = (n_{1A}^0 - n_{1B}^0)/n_0$, and the function $H(x)$ depends on the wall-interaction potential. For our choice of wall-particle interaction we have

$$H(x) = x[\exp(x) + (1/2)\int_0^1 dy \exp(xy^{\frac{3}{2}})]$$

The surface tension σ between the two phases 1 and 2 is related to the profile of the planar interface separating the equilibrium phases [28]. For our system this can be written as

$$\sigma = m \int dz \{(d[n\phi]/dz)^2 - (dn/dz)^2\} \tag{4}$$

[28,29], where $n(z)\phi(z) = n_A(z) - n_B(z)$, $n(z) = n_A(z) + n_B(z)$, and $m = (1/12)\int d\mathbf{r} V(r) r^2$, with $V(r)$ the long-range repulsive interaction between the two species. (NB. Here z stands

for the distance from the center of a planar interface separating the two bulk phases.) As remarked in [19] and is well-known for these systems [28], $\phi(z)$ is well represented as $\phi_0 \tanh(z/2\xi)$, where ξ is a correlation length that characterizes the interface thickness. Furthermore, the total density profile $n(z)$ is well characterized as $n_0[1-\delta\mathrm{sech}(z/2\xi)]$, where ϕ_0 and n_0 are the values of the order parameter and density far from the interface. With these considerations, the surface tension between phases 1 and 2 can be computed as:

$$\sigma = \frac{k_B T_c n_0 G(\phi_0, \delta)}{4\gamma^2 \xi}. \tag{5}$$

Here γ^{-1} is the range of the inter-species potential $V(r) = \alpha\gamma^3 U(\gamma r)$, where, as in [19], we use $U(x) = \pi^{-\frac{3}{2}} \exp(-x^2)$ (note that $k_B T_c = n_0\alpha/2$ [19]). The function $G(\phi_0, \delta)$ has a simple algebraic form,

$$G(\phi_0, \delta) = (2/3)\phi_0^2 - (1/3)\delta^2 + (7/15)\delta^2\phi_0^2 - (\pi/4)\delta\phi_0^2$$

Therefore, we obtain the desired ratio for Young's condition as

$$\frac{\sigma}{\gamma_2 - \gamma_1} = \frac{T_c}{T}\frac{G(\phi_0, \delta)}{\phi_0}\frac{1}{4\gamma^2\xi r_0 H(\beta W_0)}. \tag{6}$$

The physical quantities ξ, δ and ϕ_0 have been obtained in simulations of the interface profile at $T/T_c = 0.6$ [19] as $\xi \simeq 1.5\gamma^{-1}$, $\phi_0 \simeq 0.8$, $\delta \simeq 0.2$, and we set $r_0 = \gamma^{-1}$. Recall that we vary the surface potential strength W_0, and keep other parameters fixed as specified above. We then estimate Young's condition as corresponding to $\beta W_0^Y \simeq 0.071$. We have performed simulations with W_0/W_0^Y ranging from 0.67 to about 5. The size of the system was $60 \times 60 \times 120$ in units of the potential range γ^{-1}, and the number of particles used was approximately $N = 2.5 \times 10^6$. For each value of W_0 we averaged the results of 12-15 independent runs, wherever statistical averaging was required. In the figures presented below the unit of length is γ^{-1} and the unit of time is the mean-free time between collisions $\tau = \lambda/c$, $\lambda = (2^{\frac{1}{2}}\pi n d^2)^{-1}$, $c = (2k_B T/m)^{\frac{1}{2}}$, where n is the overall particle density, d is the hard sphere diameter and T is the temperature.

IV. NUMERICAL RESULTS

As discussed in the previous section, $W_0/W_0^Y < 1$ and $W_0/W_0^Y > 1$ should correspond to the PW and CW cases, respectively. In our subsequent discussion, we will refer to $W_0/W_0^Y < 1$ as the weak-field case, and $W_0/W_0^Y > 1$ as the strong-field case. Of course, we should stress that there are additional entropic effects, which have not been accounted for in our calculation. In general, this would raise the critical surface field for transition from PW to CW morphologies.

Fig. 1 shows 3-dimensional snapshots of the evolution for $W_0/W_0^Y = 0.67$ at times $t = 60, 120$ and 180. The wall is located at $z = 0$ (extreme right) and preferentially attracts A, though it is not completely wetted by A. The enrichment layer (in A) at the surface is followed by a depletion layer in A; and this layered structure deforms continuously into the bulk, as has been seen in various earlier studies for both the diffusive [14], [4] and hydrodynamic [17] cases. Fig. 2 shows laterally-averaged profiles $\phi_{av}(z,t)$ vs. z (depth from the surface) for the evolution depicted in Fig. 1 at times $t = 50, 100, 200$ and 275. These profiles are obtained by averaging the order parameter profiles in the direction parallel to the surface – analogous to the corresponding experimental situation [3]. There is a systematic profile at the surface, which decays to zero (due to isotropic phase separation) in the bulk. The systematic surface profile propagates into the bulk with the passage of time. Furthermore, the degree of enrichment diminishes as isotropic phase separation in the bulk destroys the layered structure at the surface.

To characterize the morphology of the surface layer, Fig. 3 plots the first and second zeros of the laterally-averaged profiles as a function of time. After an initial transient regime, the position of the first and second zeros grow approximately linearly in time. The linear growth of the first zero results from hydrodynamic draining of the preferred material to the surface through bulk tubes which make contact with the surface layer. This is in accordance with the observation of Tanaka and Araki [17], and the mechanism for this was discussed in subsection 2.2. Additionally, it is reasonable to expect that the overall composition of

the first and second layers should be comparable with the average composition. Thus, we expect the second zero, $R_2(t)$, to exhibit the same scaling behavior as the first zero, $R_1(t)$.

Next we consider the evolution for the (very) strong-field case, where the surface is completely wetted by the preferred component. Fig. 4 shows 3-dimensional evolution pictures for the case $W_0/W_0^Y = 4$ at $t = 60, 120, 180$. Notice the perfectly layered structure at the surface. Figs. 1 and 4 should be compared with analogous pictures for the diffusive problem [4]. Fig. 5 shows the corresponding laterally-averaged profiles at $t = 50, 100, 200$ and 275. The broad features are the same as in Fig. 2, but the level of enrichment (depletion) of A in the surface layer (next-to-surface layer) is much higher. This layered structure evolves more slowly in time because the bulk domains have not established contact with the surface layer on the time-scales of our simulation. Thus, growth of the wetting layer occurs only through diffusive transport of A from the bulk through the depletion layer in A. There are two regimes for diffusive growth [13]. In the first regime, the attractive force due to the surface potential gives a potential-dependent growth law. In the asymptotic regime, the chemical potential gradient between the domains in the bulk and the flat wetting layer gives rise to an asymptotic growth law $R_1(t) \sim t^{1/3}$, provided that the preferred component is not the majority component. The crossover time between the first and second regimes depends on the strength and range of the surface potential [13]. In the present case, we have a long-ranged surface potential ($V(z) \sim z^{-3}$). The corresponding exponent for the potential-dependent growth regime is $\phi = 0.2$ (in general, $\phi = \frac{1}{n+2}$ for $V(z) \sim z^{-n}$ [13]); and the asymptotic exponent for diffusive growth is $\phi = 1/3$.

The growth of the location of the first and second zeros of the laterally-averaged profile for this case is shown as a function of $t^{1/3}$ in Fig. 6. This plot is consistent with growth driven by the chemical potential gradient between curved domains in the bulk and the flat wetting layer. As we have remarked earlier, the strong layering inhibits the operation of draining modes to the surface layer, which would give rise to the expected asymptotic behavior $R_1(t) \sim t$. We also show in Fig. 7 the growth of the first zero of the laterally-averaged profiles for all cases that we studied. The sharpness of the transition between the

growth in the weak and strong field cases is remarkable and is in very good agreement with our analysis of the partial and complete wetting morphologies.

V. DISCUSSION

Our mesoscopic-level modeling is in terms of coupled Vlasov-Boltzmann equations for binary hard-sphere mixtures with additional long range interactions. The major advantage of our modeling is that it enables the study of much larger systems than those accessible in MD simulations. At the same time, we are still able to identify scales and parameters in terms of microscopic quantities – in contrast to modeling via coarse-grained partial differential equations.

The present work has focused on the morphology and temporal evolution of surface-directed spinodal decomposition waves in critical binary fluids. We have considered parameter values where the surface is either partially wet or completely wet in equilibrium. It is not our argument that the asymptotic behavior of these two cases is different. Rather, we would like to stress the appearance of long-lived transient regimes which are critically dependent on the morphology. These should be of relevance in the interpretation of experiments. A confusing range of exponents have been reported in various studies and we believe that the present work helps systematize these exponents.

(a) Let us first focus on the diffusive problem. These are relevant for binary fluids at early times. Furthermore, if the composition of the binary fluid is such that the domain morphology is not continuous, domain growth again proceeds through diffusive processes [1]. For cases where the preferred component is the minority component, the wetting layer exhibits a potential-dependent growth law, $R_1(t) \sim t^{\frac{1}{n+2}}$ for $V(z) \sim z^{-n}$ [13], which crosses over to a universal growth law, $R_1(t) \sim t^{1/3}$. The crossover time depends on the surface field strength and the wetting-layer morphology. For cases where the preferred component is the majority component, a potential-dependent growth law applies for all time [13].

(b) Let us next consider the hydrodynamic case. For strongly off-critical compositions,

hydrodynamic growth modes are inactive because of the discontinuous domain morphology. As we have stated earlier, the results quoted in (a) apply for this case. For bicontinuous bulk morphologies, wetting-layer growth can be characterized as follows. There is an early-time growth ("fast mode", with $L_s(t) \sim t^{3/2}$) associated with the formation of a coating layer [7,9]. Subsequently, we expect the wetting layer to exhibit the diffusive behavior outlined in (a) above. The asymptotic regime ($R_1(t) \sim t$) is accessed when the bulk establishes contact with the wetting layer, enabling the activation of hydrodynamic draining modes. Again, the crossover to the asymptotic behavior is dependent on the surface field strength and surface morphology, and can be substantially delayed for strongly-layered surface structures.

ACKNOWLEDGEMENTS

S.P. is grateful to Department of Mathematics, Rutgers University, where this work was initiated. Research supported in part by NSF Grant DMR-9813268 and AFOSR Grant F49620-98-1-0207.

REFERENCES

† Present address: Lawrence Livermore National Laboratory, P. O. Box 808, Livermore, CA 94550. Email: bastea2@llnl.gov

[1] For reviews, see K. Binder, in *Materials Science and Technology, Vol. 5: Phase Transformations in Materials* (ed. R.W. Cahn, P. Haasen and E.J. Kramer), p. 405, VCH, Weinheim, New York (1991); A.J. Bray, Adv. Phys. **43**, 357 (1994); J.D. Gunton, M. San Miguel and P.S. Sahni, in *Phase Transitions and Critical Phenomena, Vol. 8*, C. Domb and J.L. Lebowitz, editors, Academic Press, New York (1983); P.F. Fratzl, J.L. Lebowitz, O. Penrose and J. Amar, Phys. Rev. B **44**, 4794 (1991).

[2] R.A.L. Jones, L.J. Norton, E.J. Kramer, F.S. Bates and P. Wiltzius, Phys. Rev. Lett. **66**, 1326 (1991).

[3] For a review of experimental techniques and results for this problem, see G. Krausch, Mater. Sci. Eng. R. **R14**, 1 (1995).

[4] For a review of modeling and numerical simulations of this problem, see S. Puri and H.L. Frisch, J. Phys. Condens. Mat. **9**, 2109 (1997); K. Binder, J. Non-Equil. Thermody. **23**, 1 (1998).

[5] E.D. Siggia, Phys. Rev. A **20**, 595 (1979).

[6] P. Guenoun, D. Beysens and M. Robert, Phys. Rev. Lett. **65**, 2406 (1990); Physica A **172**, 137 (1991).

[7] P. Wiltzius and A. Cumming, Phys. Rev. Lett. **66**, 3000 (1991); A. Cumming, P. Wiltzius, F.S.Bates and J.H. Rosedale, Phys. Rev. A **45**, 885 (1992).

[8] B.Q.Shi, C. Harrison and A. Cumming, Phys. Rev. Lett. **70**, 206 (1993); C. Harrison, W. Rippard and A. Cumming, Phys. Rev. E **52**, 723 (1995).

[9] H. Tanaka, Phys. Rev. Lett. **70**, 53, (1993); Europhys. Lett. **24**, 665 (1993); Phys. Rev.

E **54**, 1709 (1996); H. Tanaka and T. Sigekuzi, Phys. Rev. E **52**, 829 (1995).

[10] T. Young, Phil. T. R. Soc. Lond. **95**, 69 (1805); see also Ref. [28].

[11] A.J. Liu, D.J. Durian, E. Herbolzheimer and S.A. Safran, Phys. Rev. Lett. **65**, 1897 (1990).

[12] J.W. Cahn, J. Chem. Phys. **66**, 3667 (1977).

[13] S. Puri and K. Binder, Phys. Rev. Lett. **86**, 1797 (2001); H.W. Diehl and S. Puri, in preparation.

[14] For example, see S. Puri and K. Binder, Phys. Rev. A **46**, R4487 (1992); Phys. Rev. E **49**, 5359 (1994); J. Stat. Phys. **77**, 145 (1994); S. Puri, K. Binder and H.L. Frisch, Phys. Rev. E **56**, 6991 (1997).

[15] P. Keblinski, W.-J. Ma, A. Maritan, J. Koplik and J.R. Banavar, Phys. Rev. E **47**, R2265 (1993); Phys. Rev. Lett. **72**, 3738 (1994); W.-J. Ma, P. Keblinski, A. Maritan, J. Koplik and J.R. Banavar, Phys. Rev. E **48**, R2362 (1993).

[16] H. Chen and A. Chakrabarti, Phys. Rev. E **55**, 5680 (1997).

[17] H. Tanaka and T. Araki, Europhys. Lett. **51**, 154 (2000).

[18] S. Toxvaerd, Phys. Rev. Lett. **83**, 5318 (1999).

[19] S. Bastea and J.L. Lebowitz, Phys. Rev. Lett. **78**, 3499 (1997).

[20] S. Chapman and T.G. Cowling, *The Mathematical Theory of Non-uniform Gases*, (Cambridge University Press, London, 1970).

[21] S. Bastea, R. Esposito, J.L. Lebowitz and R. Marra, J. Stat. Phys. **101**, 1087 (2000).

[22] S. Bastea, Comp. Phys. Comm. bf 121-122, 270 (1999).

[23] G.A. Bird, *Molecular Gas Dynamics*, (Clarendon Press, Oxford, 1976).

[24] C.K. Birdsall and A.B. Langdon, *Plasma Physics Via Computer Simulation*, (McGraw-Hill Book Company, New York, 1985).

[25] J.P. Hansen and I.R. McDonald, *Theory of Simple Liquids*, Academic Press, Orlando (1986).

[26] C. Cercignani, R. Illner and M. Pulvirenti, *The Mathematical Theory of Dilute Gases*, Springer-Verlag, New York (1994).

[27] H.J.C. Berendsen, J.P.M. Postma, W.F. van Gunsteren, A. Nicola and J.R. Haak, J. Chem. Phys. **81**, 3684 (1984).

[28] J.S. Rowlinson and B. Widom, *Molecular Theory of Capillarity*, Clarendon Press, Oxford (1982).

[29] S. Bastea, *Ph.D. Thesis*, Rutgers University, New Brunswick (1997).

FIGURES

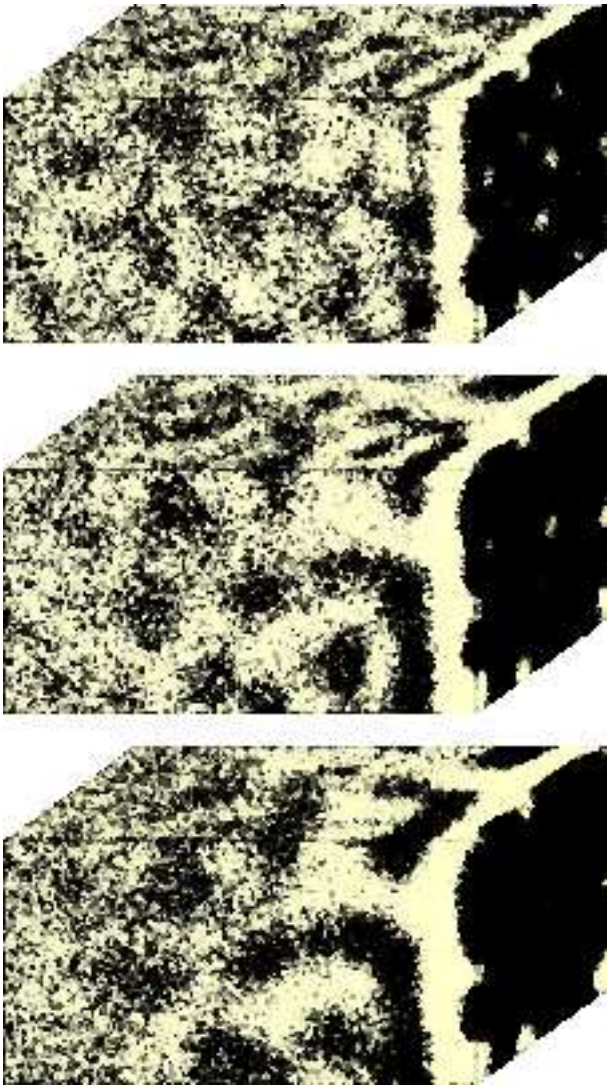

FIG. 1. Snapshots of the evolution after a critical quench for a weak-field case $W_0/W_0^Y = 0.67$. The equilibrium surface morphology is partially wet. The times corresponding to the pictures are (from top to bottom) $t = 60, 120, 180$.

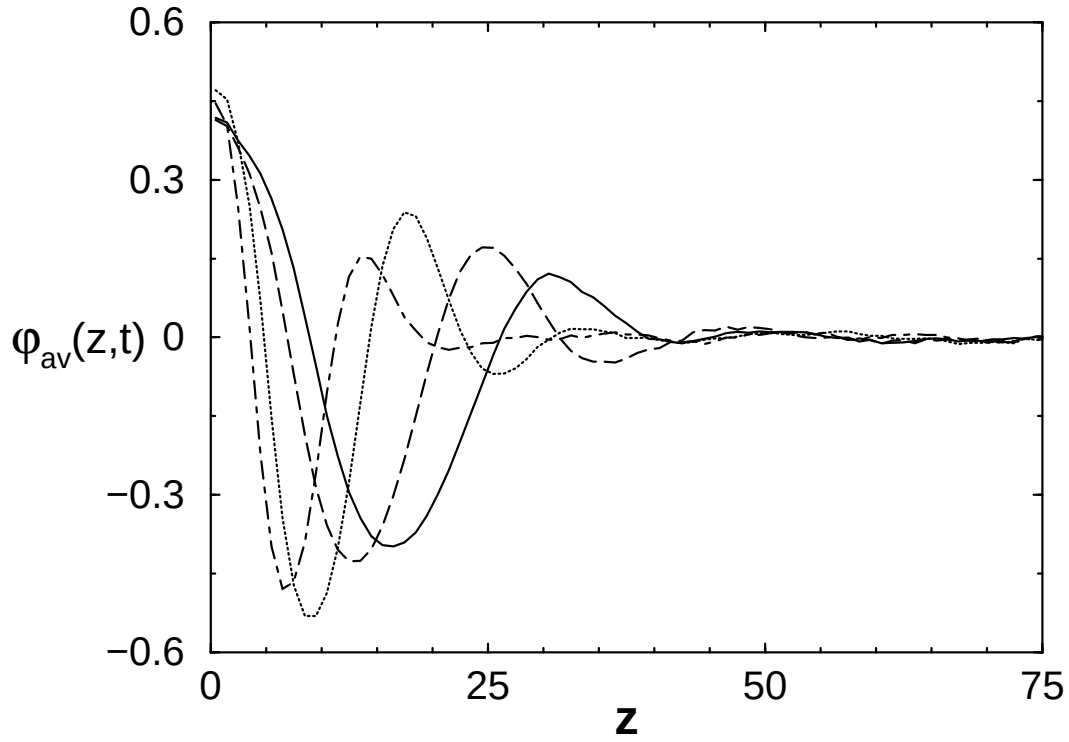

FIG. 2. Laterally-averaged order parameter profiles, $\phi_{av}(z,t)$, as a function of z, the distance from the surface. Parameter values are the same as those for the evolution depicted in Fig. 1. The evolution times are $t = 50$ (dot-dashed), 100 (dotted), 200 (dashed) and 275 (solid line).

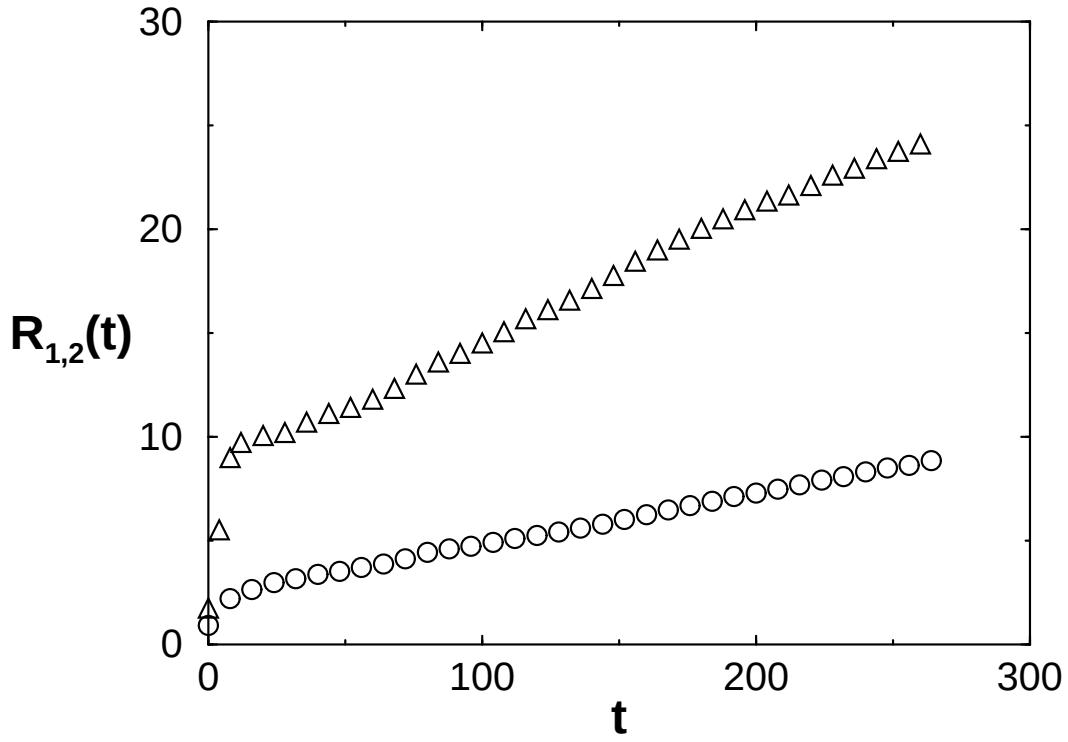

FIG. 3. Time-dependence of first zero $R_1(t)$ (circles); and second zero $R_2(t)$ (triangles), of the laterally-averaged profiles shown in Fig. 2.

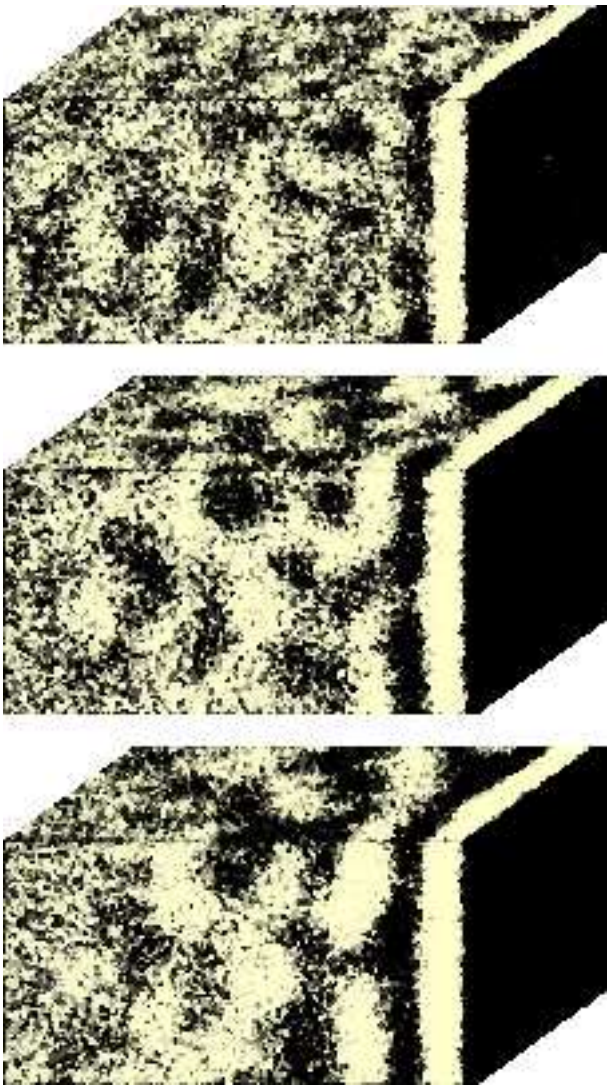

FIG. 4. Analogous to Fig. 1, but for a (very) strong-field case $W_0/W_0^Y = 4$, where the surface is completely wetted by the preferred component in equilibrium.

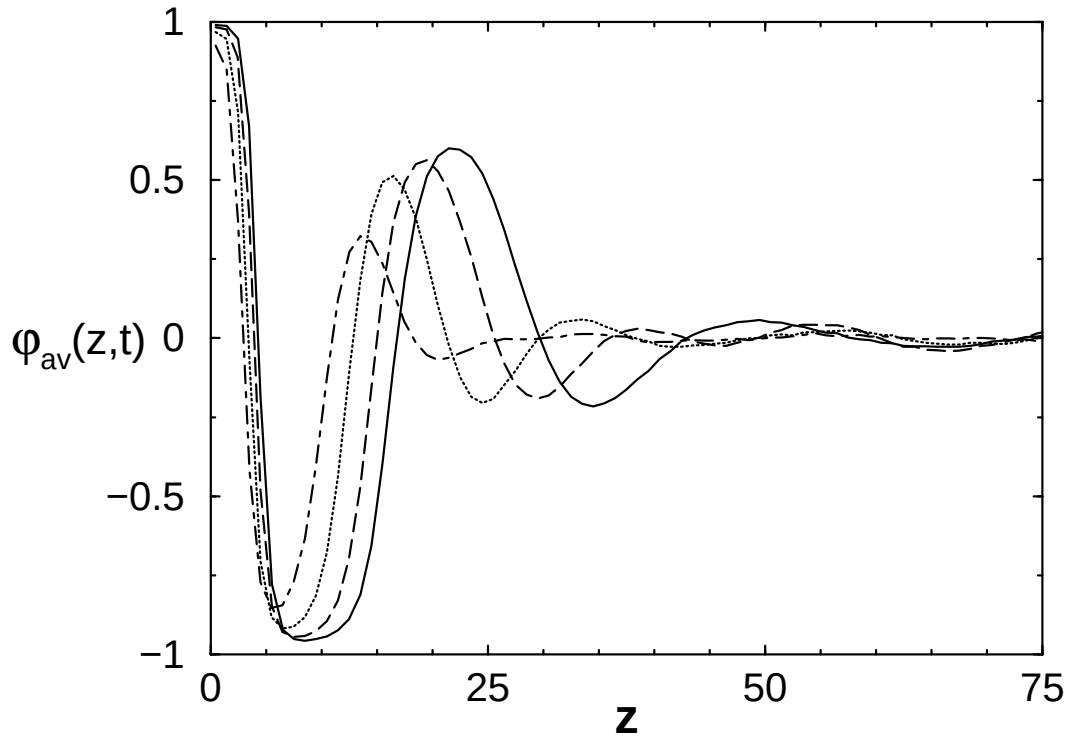

FIG. 5. Analogous to Fig. 2, but for the evolution depicted in Fig. 4 for the strong-field case. The profiles are shown at times $t = 50$ (dot-dashed), 100 (dotted), 200 (dashed) and 275 (solid line).

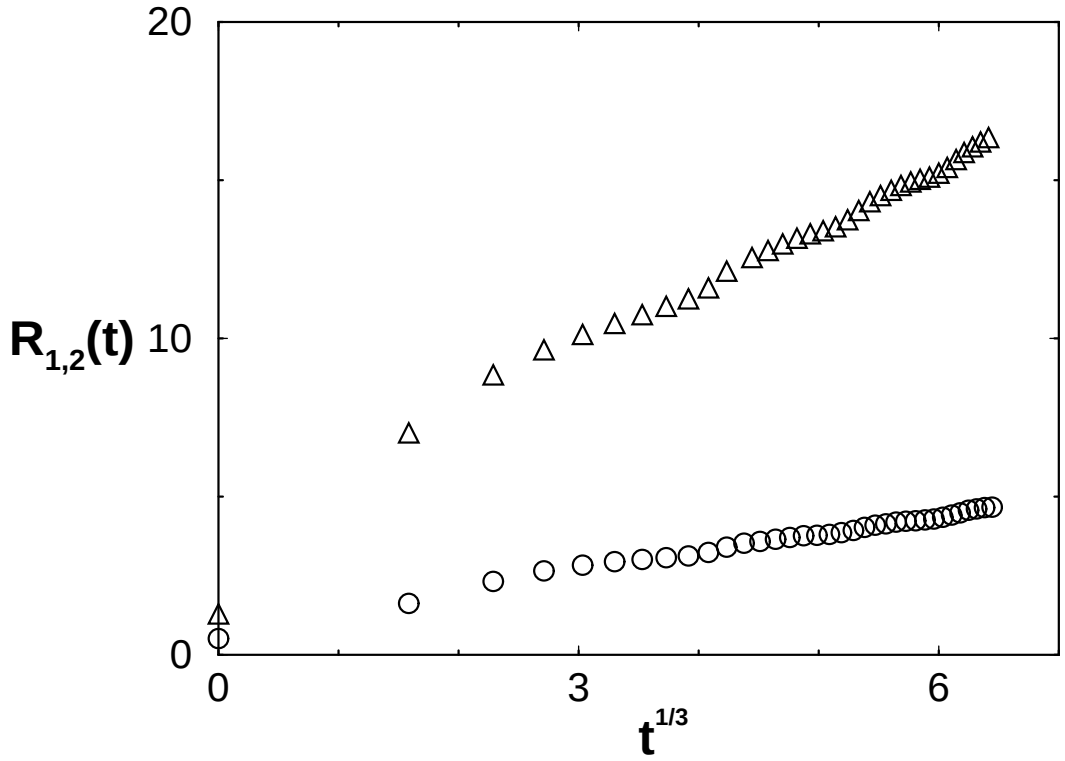

FIG. 6. Plot of first zero $R_1(t)$ vs. $t^{1/3}$ (circles); and second zero $R_2(t)$ vs. $t^{1/3}$ (triangles), of the laterally-averaged profiles shown in Fig. 5.

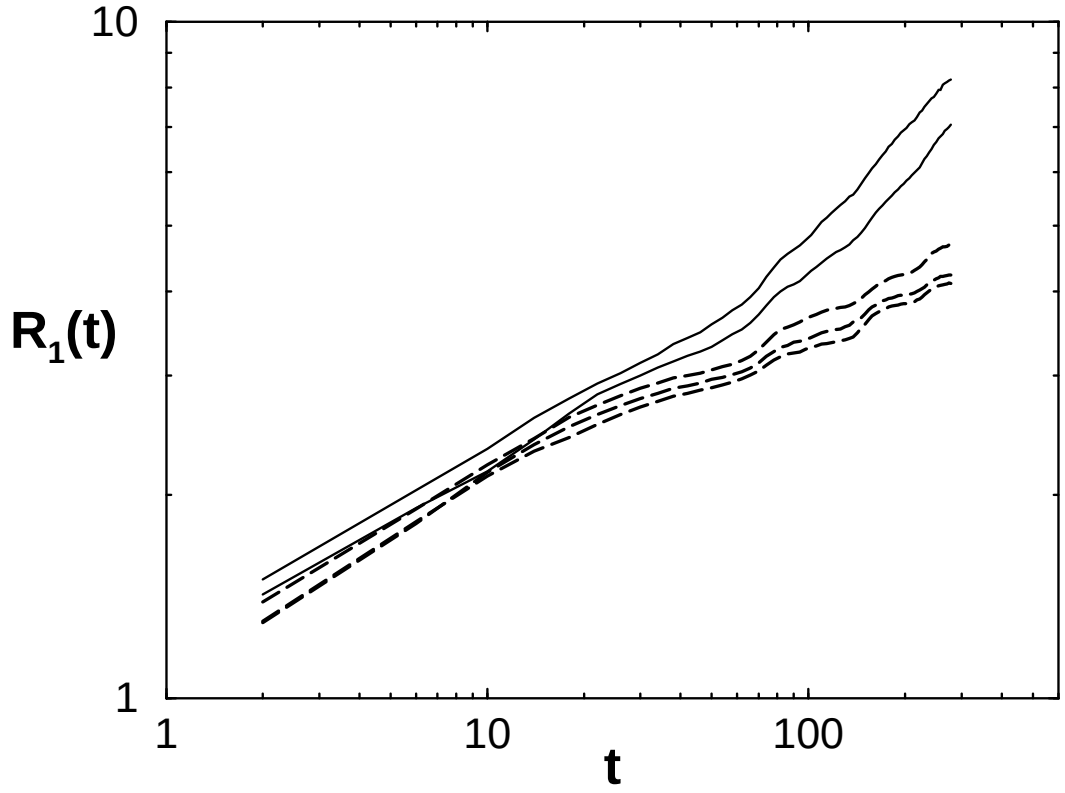

FIG. 7. Time evolution of the first zero, R_1, of the laterally-averaged profile for all cases studied: from top, $W_0/W_0^Y = 0.67, 1.33, 2.67, 4.0$ and 5.33.